2012-05-07

Accurate ab initio potential energy surfaces for the (3)A '' and (3)A ' electronic states of the O(P-3) plus HBr system

JOURNAL OF CHEMICAL PHYSICS, MELVILLE, v. 136, n. 17, supl. 1, Part 2, pp. 1861-1870, MAY 7, 2012
http://www.producao.usp.br/handle/BDPI/32521

Accurate ab initio potential energy surfaces for the 3A″ and 3A′ electronic states of the O(3P)+HBr system

Antonio G. S. de Oliveira-Filho, Fernando R. Ornellas, and Kirk A. Peterson

Citation: J. Chem. Phys. **136**, 174316 (2012); doi: 10.1063/1.4705428
View online: http://dx.doi.org/10.1063/1.4705428
View Table of Contents: http://jcp.aip.org/resource/1/JCPSA6/v136/i17
Published by the American Institute of Physics.

Accurate *ab initio* potential energy surfaces for the $^3A''$ and $^3A'$ electronic states of the O(^3P)+HBr system

Antonio G. S. de Oliveira-Filho,[1,a)] Fernando R. Ornellas,[1] and Kirk A. Peterson[2]
[1]*Departamento de Química Fundamental, Instituto de Química, Universidade de São Paulo, Av. Prof. Lineu Prestes, 748, São Paulo, São Paulo 05508-000, Brazil*
[2]*Department of Chemistry, Washington State University, Pullman, Washington 99164-4630, USA*

(Received 14 February 2012; accepted 9 April 2012; published online 7 May 2012)

In this work, we report the construction of potential energy surfaces for the $^3A''$ and $^3A'$ states of the system O(^3P) + HBr. These surfaces are based on extensive *ab initio* calculations employing the MRCI+Q/CBS+SO level of theory. The complete basis set energies were estimated from extrapolation of MRCI+Q/aug-cc-V*n*Z(-PP) (n = Q, 5) results and corrections due to spin-orbit effects obtained at the CASSCF/aug-cc-pVTZ(-PP) level of theory. These energies, calculated over a region of the configuration space relevant to the study of the reaction O(^3P) + HBr → OH + Br, were used to generate functions based on the many-body expansion. The three-body potentials were interpolated using the reproducing kernel Hilbert space method. The resulting surface for the $^3A''$ electronic state contains van der Waals minima on the entrance and exit channels and a transition state 6.55 kcal/mol higher than the reactants. This barrier height was then scaled to reproduce the value of 5.01 kcal/mol, which was estimated from coupled cluster benchmark calculations performed to include high-order and core-valence correlation, as well as scalar relativistic effects. The $^3A'$ surface was also scaled, based on the fact that in the collinear saddle point geometry these two electronic states are degenerate. The vibrationally adiabatic barrier heights are 3.44 kcal/mol for the $^3A''$ and 4.16 kcal/mol for the $^3A'$ state. © *2012 American Institute of Physics*. [http://dx.doi.org/10.1063/1.4705428]

I. INTRODUCTION

Hydrogen bromide (HBr), a relatively inactive form of bromine in the stratosphere, is the principal bromine sink compound for ozone loss chemistry.[1] Along with other processes, active atomic bromine can be regenerated by the reaction O(^3P) + HBr → OH + Br.[2] An interesting aspect of this reaction is that it is relatively simple in the sense that it can be studied in detail both theoretically and experimentally. Thermal rate constants have been measured by several groups over the combined temperature range of 221–554 K; these data are in good agreement and show a slight curvature in the Arrhenius plot,[3–7] as first noted by Nava and co-workers.[6] Also a significant number of literature results are concerned with product state distributions, focusing on the population inversion present in the OH vibrational branching ratio[3,8] and in its rotational population distribution.[9–11] The observed preference to dispose the energy in product excitation is characteristic of the kinematic constraints for the transfer of a light atom between two heavy ones (H + LH′ → HL + H′).

A central feature in the theoretical description of chemical reactions in a quantitative way is the construction of an accurate potential energy surface (PES), and extensive high-level calculations are usually employed to generate energies that can be used to obtain an explicit function for the potential. To the best of our knowledge, this kind of study has not been conducted yet on the O(^3P) + HBr system, despite the fact that several investigations on the O(^3P) + HCl reaction have been reported in the literature.[12–16] The first studies reporting calculations of rate constants for the triplet O + HBr reaction were based on the bond-energy-bond-order (BEBO)[4,5,17,18] method and on London-Eyring-Polanyi-Sato (LEPS)[19,20] PESs adjusted to reproduce experimental kinetic data. Urban and Staemmler[21] built an extended-LEPS surface based on about fifty coupled electron pair approximation (CEPA) points and found an activation energy of 10 kcal/mol, overestimating the recommended value of 3 kcal/mol.[22] Better agreement with the empirical value was found by Jalbout[23] using a variety of density functionals to calculate transition state geometries, activation barriers, and reaction energies. While, unlike the early studies, these latter two works accounted for the fact that the reaction does not necessarily occur in a collinear minimum energy path, none of them considered the possibility of van der Waals wells in the entrance and exit channels.

In this paper our major focus is the construction of reliable PESs for an accurate description of the O(^3P) + HBr reaction dynamics in the $^3A''$ and $^3A'$ electronic states. Here, we followed a procedure similar to the one used by Ramachandran and Peterson[15] for the O(^3P) + HCl reaction, which proved to yield very good thermal rates using either transition state theory or pure quantum mechanical rates when compared to experimental data.[24]

II. COMPUTATIONAL DETAILS

The *ab initio* points used to generate the PESs were calculated in the following way. First a dynamically weighted[25]

a)Electronic mail: oliveira@iq.usp.br.

state averaged complete active space self-consistent field[26,27] (CASSCF) calculation was carried out using a full valence active space, excluding the *s* valence orbitals from oxygen and bromine. Three states of A′ and three states of A″ symmetries, in the C_s point group, were considered in this step. This is the smallest number of states necessary to describe the electronic degeneracy in the reactants limit ($O\,(^3P_g) + HBr\,(^1\Sigma^+) \Rightarrow {}^3A' + 2\,{}^3A''$) and in the products ($OH\,(^2\Pi) + Br\,(^2P_u) \Rightarrow 3\,{}^3A' + 3\,{}^3A''$). A weighted average of states with the β^{-1} factor set to 3 eV was used to take into account this difference between reactants and products and connect them smoothly. This was followed by an internally contracted multireference configuration interaction[28,29] (MRCI) calculation using the Davidson correction[30] (+Q) to correlate all valence electrons (1*s* of H, 2*s*2*p* of O, 4*s*4*p* of Br). These calculations employed the aug-cc-pV*n*Z basis set for hydrogen and oxygen[31,32] and the aug-cc-pV*n*Z-PP for bromine,[33,34] where $n = Q, 5$, and the (1*s*-2*p*) inner core of bromine was replaced by a relativistic pseudopotential.[33] The energies obtained with these two basis sets were then extrapolated to the complete basis set (CBS) limit using[35]

$$E(n) = E_{CBS} + B/n^3 \quad (n = 4, 5). \tag{1}$$

Spin-orbit effects were included by adding a correction calculated at the CASSCF/aug-cc-pVTZ(-PP) level using the full Breit-Pauli operator within the state interacting approach[36] where 9 singlets (4 in A' and 5 in A'' symmetry) and 18 triplet states (8 in A' and 10 in A'') were mixed.

In order to get accurate energetics, additional calculations were also carried out on the reactants, products, and other stationary points of the PES. Geometry optimizations and frequency calculations were done for the minima and transition state at the coupled cluster with single and double substitution level of theory with a perturbative estimate for connected triples[37] (CCSD(T)). More specifically, we chose a spin unrestricted variant of the CC theory that uses restricted open shell Hartree–Fock (ROHF) orbitals, known as R/UCCSD(T).[38,39] For the atomic basis, we chose the same sets and extrapolation expression used for the MRCI+Q calculations. Additive corrections to include the effect of full iterative triple and quadruple excitations, core-valence correlation, scalar relativity, and spin-orbit have been calculated at the R/UCCSD(T)/AV5Z geometry. The triple excitation correction (ΔT) was defined as the difference between R/UCCSD(T) and CCSDT[40–42] calculations using the aug-cc-pVTZ(-PP) basis set;[31,32,43] similarly, the quadruple excitation correction (ΔQ) was calculated from CCSDT and CCSDTQ[44–46] energies using the cc-pVDZ(-PP) basis set. The core-valence correlation was included at the CCSD(T) level using the aug-cc-pwCVTZ(-PP) basis set[47,48] as the difference between frozen-core calculations and those with the O 1s and Br 3*s*3*p*3*d* electrons correlated (both in the same basis set). The second-order Douglas-Kroll-Hess (DKH) Hamiltonian[49] along with the DKH-contracted basis sets,[43,50] aug-cc-pVTZ-DK, was used to include scalar relativistic effects on H and O, as well as to also correct for the pseudopotential approximation. This contribution was defined as the difference between R/UCCSD(T)/AVTZ(-PP) and DK-R/UCCSD(T)/AVTZ-DK energies within the frozen-core approximation. The last correction, for the spin-orbit effect, added the difference between non-spin-orbit and spin-orbit calculations at the CASSCF/AVTZ(-PP) level as described above. All calculations were carried out with the MOLPRO[51] suite of *ab initio* programs, while the CCSDT and CCSDTQ calculations were performed with the MRCC[52] program as interfaced to MOLPRO.

III. POTENTIAL ENERGY SURFACES

A grid defined by the internal coordinates r_{OH}, r_{HBr}, and θ_{OHBr} was used to calculate the PES:

$$\begin{aligned} r_{OH}[a_0] &= 1.35, 1.50, 1.65, 1.80, 2.00, 2.25, 2.50, \\ &\quad 2.75, 3.00, 3.25, 3.50, 4.00, 5.00, 6.00, \\ r_{HBr}[a_0] &= 2.20, 2.35, 2.50, 2.65, 2.85, 3.10, 3.35, 3.60, \\ &\quad 3.85, 4.10, 4.35, 4.85, 5.85, 6.85, \\ \theta_{OHBr}[deg] &= 179.99, 160, 140, 120, 100, 80, 60. \end{aligned}$$

Of all possible combinations, the points for which simultaneously $r_{OH} > 2.50\ a_0$ and $r_{HBr} > 3.35\ a_0$ have been not considered. This region of the configuration space, with all atoms relatively far from each other, does not contribute significantly to the description of the three-body potential, and the proximity to the atomization limit could generate some near-degeneracy-related problems that could require a CASSCF calculation with all 18 triplet states of the three separated atoms. So the number of points calculated using this grid could be reduced to 1029. These points have been used for the $^3A'$ and $^3A''$ surfaces, but for the latter an additional set of 81 points were calculated in regions close to both van der Waals minima and the transition state to improve their characterization, using a total of 1110 points for the $^3A''$ PES. Both surfaces are described in terms of a many body expansion,[53–55]

$$V(r_1, r_2, r_3) = V^{(1)} + \sum_{i=1}^{3} V^{(2)}(r_i) + V^{(3)}(r_1, r_2, r_3), \tag{2}$$

where $V^{(1)}$, $V^{(2)}(r_i)$, and $V^{(3)}(r_1, r_2, r_3)$ are, respectively, the sum of atomic energies, the two-body term, and the three-body term.

A. Two-body potentials

The two-body terms for the OH and HBr potentials were adjusted by the switched-MLJ (Modified Lennard-Jones) function of Hajigeorgiou and Le Roy,[56]

$$V^{(2)}(r) = D_e \left[\left(1 - \left(\frac{r_e}{r} \right)^6 e^{-\beta^s_{MLJ}(z) z} \right)^2 - 1 \right], \tag{3}$$

where $z = (r - r_e)/(r + r_e)$, and

$$\beta^s_{MLJ}(z) = f_s(r) \left[\sum_{m=0}^{M} \beta_m z^m - \beta_\infty \right] + \beta_\infty, \tag{4}$$

where $\beta_\infty = \ln(2D_e r_e^6 / C_6)$, and $f_s(r) = (e^{\alpha_s (r - r_s)} + 1)^{-1}$. D_e and r_e were fixed at values obtained from near-equilibrium

polynomial fits, while the parameters controlling the switching function were kept close to the authors' recommendations, namely $\alpha_s \sim 4/(r_s - r_e)$ and $r_s \sim r_{max} + 1$ a$_0$, where r_{max} was the maximum r used in the fit. The dispersion coefficient, C_6, defines the long range behavior of the function, because in the limit $r \to \infty$ the potential has the form $V(r) = -C_6/r^6$. In order to get the appropriate long range behavior, the C_6 coefficients where fixed at values obtained from experimental results for atomic polarizabilities and ionization potentials, 9.134 for OH and 32.274 for HBr, in atomic units. The final fits were adjusted to 15 points for HBr and to 14 points for OH. The root mean square errors (RMSE) were 0.035 and 0.041 kcal/mol for HBr and OH, respectively, using M = 8 for both potentials.

As in a previous work on the O + HCl system,[15] where the ClO potential was considered as purely repulsive, the BrO potential was also represented by a repulsive function to avoid unphysical minima in the $\theta_{OHBr} < 60^\circ$ region. This approach is valid because the H + BrO channel is approximately 35 kcal/mol higher in energy than the reactants, O + HBr.

B. Three-body potentials

The three-body potentials were described in terms of the reproducing kernel Hilbert space (RKHS) theory, as introduced by Ho and Rabitz.[57,58] The interpolated functions are calculated by

$$V^{(3)}(x_i, y_i, z_i) = \sum_{j=1}^{N} C_j \, Q^{6,6,2}(x_i, x_j; y_i, y_j; z_i, z_j), \quad (5)$$

$$i = 1, 2, \ldots, N,$$

where N is the number of *ab initio* points (1110 for the $^3A''$ PES and 1029 for the $^3A'$ PES), C_j are the coefficients determined using the Cholesky decomposition, and $Q^{6,6,2}$ is the three-dimensional kernel, written as the product of one dimensional kernels:

$$Q^{6,6,2} = q_1^{2,6}(x, x')q_1^{2,6}(y, y')q_2^2(z, z'), \quad (6)$$

where $x = r_{OH}$, $y = r_{HBr}$, and $z = (1 - \cos\theta_{OHBr})/2$ are the coordinates used for the interpolation. The one dimensional distance-like kernel is

$$q_1^{2,6}(x, x') = \frac{1}{14} x_>^{-7} \left\{ 1 - \frac{7}{9} \frac{x_<}{x_>} \right\}, \quad (7)$$

where $x_> = \max(x, x')$, $x_< = \min(x, x')$, and the one dimensional angle-like kernel is

$$q_2^2(x, x') = 1 + x_< x_> + 2x_<^2 x_> \left\{ 1 - \frac{1}{3} \frac{x_<}{x_>} \right\}. \quad (8)$$

A final adjustment on the PESs was to multiply the three-body potentials by scaling factors. For the $^3A''$ surface the factor value is 0.97714, found by trial and error, in order to reproduce the best estimate of the barrier height, and for the $^3A'$ surface the factor is 0.9790, chosen to make the collinear saddle point degenerate with the scaled $^3A''$ barrier. In order to illustrate the crossings at near-linear configurations at the entrance channel, and the angular dependence of the three electronic states correlating with the entrance channel, O(^3P) + HBr ($1^3A' + 2^3A''$), we display in Figure 1 a surface cut for fixed $r_{HBr} = 2.67$ a$_0$ and $\theta_{OHBr} = 179.99^\circ$, in which the van der Waals well in the lowest lying eletronic state ($^3A''$ in C_s or $^3\Sigma^-$ in $C_{\infty v}$ point group) is clearly shown. Also at $r_{OH} \sim 3$ a$_0$ there is an avoided crossing between the two lowest states with A'' symmetry that makes, at linear symmetry, the $^3\Pi$ ($^3A' + {}^3A''$ in C_s point group) the lowest lying state in the collinear barrier region, thus justifying the choice of scaling for the $^3A'$ PES. Also in Figure 1, we display the angular dependence of these electronic states in a cut of the PESs for fixed $r_{HBr} = 2.88$ a$_0$ and $r_{OH} = 2.52$ a$_0$, corresponding to a region near to the collinear saddle point. It is clear from this plot that at $\theta_{OHBr} = 180^\circ$ the lowest lying electronic state has Π symmetry, and for smaller angles this state splits into a $^3A''$, the curve with a minimum around 130°, and a $^3A'$, with its minimum at linear configurations. It is also insteresting to note that the second $^3A''$ lies about 10 kcal mol^{-1} higher in energy than the other states in this region. These curves have been calculated at the MRCI+Q/AVDZ(-PP) level of theory just to give a qualitative picture of these important features of the system.

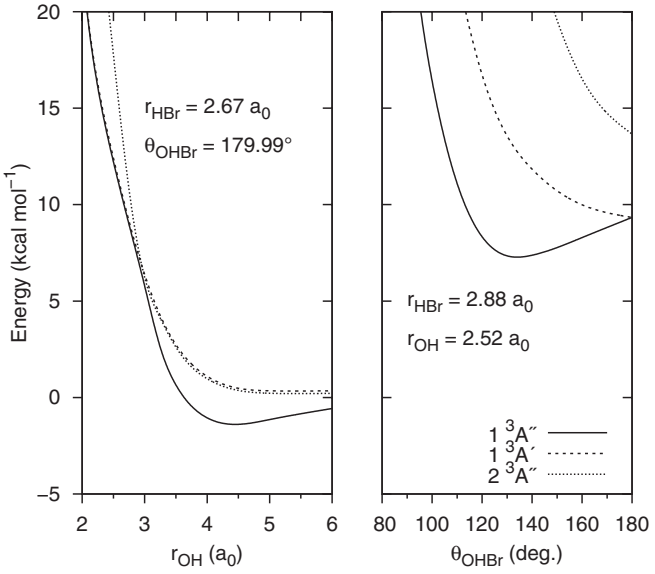

FIG. 1. Curve crossings near the entrance channel at near-linear configurations and the angular dependence of the three electronic states correlating with the O(^3P) + HBr channel. Note that at linear symmetry the $^3A'$ and $^3A''$ states are degenerate, corresponding to a $^3\Pi$ state, and the remaining $^3A'$ corresponds to a $^3\Sigma^-$ state.

IV. RESULTS AND DISCUSSION

The spectroscopic constants of the calculated (CCSD(T)/CBS without spin-orbit correction and MRCI+Q/CBS with and without spin-orbit correction) two-body potentials and the corresponding experimental values are shown in Table I. It is interesting to point out the fair agreement between the non-spin-orbit CCSD(T) and MRCI+Q results, with each other, and with the experimental values (with atomic and molecular spin-orbit contribution

TABLE I. Properties of the calculated two-body potentials compared to experimental values.

	D_e (kcal/mol)	r_e (a_0)	ω_e (cm^{-1})	$\omega_e x_e$ (cm^{-1})	α_e (cm^{-1})
		HO($^2\Pi$)			
CCSD(T)/CBS	107.1	1.8324	3745.5	83.3	0.717
MRCI+Q/CBS	106.6	1.8316	3745.1	88.7	0.758
SO-MRCI+Q/CBS	106.6	1.8316	3744.8	88.6	0.758
Experiment[a]	107.05[b] (107.16)[c]	1.8324	3737.8	84.9	0.724
		HBr($^1\Sigma^+$)			
CCSD(T)/CBS	93.0	2.6816	2646.2	44.5	0.228
MRCI+Q/CBS	92.7	2.6805	2648.4	40.9	0.248
SO-MRCI+Q/CBS	89.4	2.6812	2649.0	41.7	0.238
Experiment[d]	90.37 (93.88)[c]	2.6729	2649.3	45.4	0.233
		BrO($^2\Pi$)			
CCSD(T)/CBS	58.1	3.2483	734.0	4.57	0.0035
MRCI+Q/CBS	56.9	3.2558	722.4	4.50	0.0036
SO-MRCI+Q/CBS	54.5	3.2509	727.8	4.59	0.0036
Experiment[e]	57.0[f] (59.3)[c]	3.2451 3.2516[g]	732.9 725.4[g]	4.65 4.65[g]	0.0036 0.0036[g]

[a]Reference 59 unless otherwise noted.
[b]Reference 60.
[c]Atomic and molecular spin-orbit removed from experimental results.
[d]Reference 61.
[e]Reference 62 unless otherwise noted.
[f]Reference 63.
[g]Average for $X_1\ ^2\Pi_{3/2}$ and $X_2\ ^2\Pi_{1/2}$ states, values from Ref. 62.

to the dissociation energies removed). The inclusion of spin-orbit effects on the MRCI+Q/CBS potential energy curves slightly changes the spectroscopic constants, which are found to be in good agreement with experiment. The main impact of this correction occurs in the dissociation energies of HBr and BrO, due the large atomic SO splitting of bromine. The calculated values of D_e for these molecules are 89.4 kcal/mol and 54.5 kcal/mol, differing from experiment by 0.97 kcal/mol and 2.5 kcal/mol, respectively. The quality of the present PESs is not affected by this relatively large error in the BrO potential because we are not interested in a study of the H + BrO channel. Another way to test the quality of our calculations is the comparison between the calculated and experimental exoergicities for the reaction $O(^3P)$ + HBr → OH + Br. We obtained the value of −15.7 kcal/mol, in good agreement with the experimental value, ΔE_0 = −15.14 kcal/mol.[60,61] Certainly the remaining discrepancies between *ab initio* and experimental results would be minimized if higher-order and core-valence correlation, as well as scalar relativistic effects on the light atoms were considered, but the accuracy obtained at the present level of theory is satisfactory. We note, however, that a more detailed calculation taking into account these small contributions was done for the barrier height.

Keeping in mind that the principal aim of this work is the construction of accurate PESs for the study of the $O(^3P_g)$ + HBr reaction, it is important to point out that in this system the reactants have three-fold degeneracy ($2\ ^3A' + {}^3A''$ for bent configurations or $^3\Sigma^- + {}^3\Pi$ for linear geometries) thus leading to three reactive surfaces, as discussed by Urban and Staemmler.[21] However for the isovalent reaction (O + HCl) it is known that only the $^3A''$ and $^3A'$ surfaces are relevant, the latter being important only at high temperatures due to its higher barrier.[15,24] For this reason we restricted our study to the lowest-lying $^3A''$ and $^3A'$ electronic states.

The geometries and harmonic frequencies of the stationary points on the $^3A''$ PES are shown in Table II. The CCSD(T) results were obtained directly from MOLPRO using its optimization and frequency routines, the MRCI+Q results came from polynomial fits to grids of single-point energies close to the stationary points, and the PES and SO-PES correspond to the values obtained using functions adjusted to the expression in Eq. (2), without and with spin-orbit correction. In general, all methods yield very consistent results, confirming the quality of the interpolation and justifying the use of coupled cluster calculations to get an accurate estimate of the barrier height. The entrance van der Waals (vdW) minimum (O–HBr) is a very shallow well, about −1.68 kcal/mol deep, relative to the reactants, with linear geometry and bond lengths of 4.469 a_0 for r_{OH}, and 2.684 a_0 for r_{HBr} at the MRCI+Q/CBS level of theory. This structure can be understood as an oxygen atom interacting with a hydrogen bromide molecule, weakly bonded with a perturbed HBr bond that is 0.003 a_0 longer and with a stretching frequency of about 13 cm^{-1} less than the free HBr molecule. The CCSD(T) results with the AV5Z basis set are very similar to the corresponding MRCI+Q values, with an r_{OH} bond 0.080 a_0 shorter, an r_{HBr} bond 0.002 a_0 longer, and a well depth of −1.43 kcal/mol. For the product-side vdW minimum, there is also a concordance between MRCI+Q and CCSD(T), despite the fact that at this geometry there is strong multireference character, with four reference coefficients larger than 0.1 (0.72,0.43,0.40,0.17). The major difference between these levels of theory is that MRCI+Q/AV5Z predicts an r_{HBr} bond length 0.112 a_0 longer than the value for CCSD(T)/AV5Z, and this discrepancy is also visible in the harmonic frequencies. Despite all that, the two methodologies agree on the relative energy of this structure, −20.49 kcal/mol for MRCI+Q/CBS and −21.04 at the CCSD(T)/AV5Z level (relative to reactants). Comparing the energy of this vdW minimum to the products asymptotic limit, we have a well much deeper than the one found in the entrance channel, −6.55 kcal/mol and −7.08 kcal/mol for MRCI+Q and CCSD(T), respectively. This relative stability is reduced to −3.76 kcal/mol by the inclusion of spin-orbit effects, due to the large shift in the products energy in the SO-PES. For the transition state, the geometries and frequencies obtained with MRCI+Q and CCSD(T) are in good agreement. It is important to note that the minimum energy saddle point in the $^3A''$ electronic state is a bent structure with a θ_{OHBr} angle of 135.4°, a fact that was not considered in the early works based on collinear minimum energy paths. The MRCI+Q transition state energy is about 0.6 kcal/mol higher than the value predicted by CCSD(T) calculations.

As mentioned in Sec. II, we performed some benchmark calculations to establish accurate relative energies for the stationary points, with special interest in the transition state. The contributions of triple and quadruple excitations, core-valence correlation, scalar relativistic, and spin-orbit effects to the

TABLE II. Properties of the stationary points of the $^3A''$ PES (unscaled) as a function of the basis set and the level of theory.

Method	ΔV (kcal/mol)	r_{OH} (a_0)	r_{HBr} (a_0)	θ_{OHBr} (deg)	ω_s (cm^{-1})	ω_a (cm^{-1})	ω_b (cm^{-1})
			O–HBr (Reactant-side well)				
MRCI+Q/AVQZ	− 1.81	4.450	2.685	180	75.7	2653.6	141.9
MRCI+Q/AV5Z	− 1.74	4.459	2.684	180	74.1	2652.7	141.5
MRCI+Q/CBS	− 1.68	4.469	2.684	180	72.6	2652.7	140.9
PES	− 1.65	4.483	2.684	180	70.9	2635.5	138.6
SO-PES	− 1.56	4.477	2.685	180	70.8	2635.9	141.9
R/UCCSD(T)/AVQZ	− 1.49	4.364	2.686	180	80.2	2624.4	141.0
R/UCCSD(T)/AV5Z	− 1.43	4.379	2.686	180	...	...	...
			Transition State				
MRCI+Q/AVQZ	6.34	2.589	2.871	136.4	1344.2	1332.7*i*	243.2
MRCI+Q/AV5Z	6.44	2.591	2.871	135.9	1356.7	1332.0*i*	242.4
MRCI+Q/CBS	6.55	2.593	2.871	135.4	1369.8	1331.3*i*	241.7
PES	6.59	2.598	2.871	134.8	1422.6	1314.7*i*	248.4
SO-PES	6.55	2.608	2.868	135.7	1400.6	1294.7*i*	232.1
R/UCCSD(T)/AVQZ	5.80	2.587	2.869	136.9	1367.6	1302.5*i*	231.8
R/UCCSD(T)/AV5Z	5.86	2.590	2.869	136.1	...	...	...
			OH–Br (Product-side well)				
MRCI+Q/AVQZ	− 19.98	1.841	4.866	65.8	3691.3	225.9	583.2
MRCI+Q/AV5Z	− 20.49	1.840	4.856	65.8	3697.5	229.1	604.6
MRCI+Q/CBS	− 20.57	1.839	4.851	65.8	3701.0	230.5	605.3
PES	− 20.57	1.839	4.854	65.6	3698.4	229.3	576.4
SO-PES	− 20.96	1.838	4.880	66.4	3689.2	206.4	567.3
R/UCCSD(T)/AVQZ	− 20.88	1.839	4.751	62.4	3705.3	321.1	676.2
R/UCCSD(T)/AV5Z	− 21.04	1.838	4.744	62.4	...	...	...

energy profile of the $^3A''$ PES are summarized in Table III. All values are relative to the reactants energy. From these values one can see that the barrier height increases with the basis set size, and the most important contribution for this value is due to triple excitations, followed by the Douglas-Kroll-Hess correction and quadruple excitations. Core-valence correlation and the spin-orbit interaction lead to small effects on the barrier height, so the best estimate value for this property is 5.01 kcal/mol, 0.91 kcal/mol smaller than the CCSD(T)/CBS value, and 1.54 kcal/mol lower than the MRCI+Q/CBS+SO estimate. It is interesting to point out that all contributions are small for all stationary points, except the high-order correlation in the product-side vdW minimum and the spin-orbit effect in the products. As mentioned before, the products vdW well has a strong multireference character and in this case a single-determinant based description is less appropriate. The large spin-orbit splitting of the bromine atom is responsible for the lowering of 3.29 kcal/mol in the energy of the products and it has minor effects on the rest of the surface.

The final $^3A''$ PES had its three-body potential scaled in order to match the barrier height with the best estimate value of 5.01 kcal/mol, and since in the collinear saddle point the $^3A'$ and $^3A''$ electronic states are degenerate, the scaling factor of the $^3A'$ was chosen in a way to make the two scaled PESs degenerate in the collinear saddle point. In Table IV are displayed the properties of the saddle points on the scaled and unscaled $^3A''$ and $^3A'$ PESs. The scaling shortens the r_{HBr} bond distance by 0.019 a_0, increases the r_{OH} distance by

TABLE III. Benchmark energy calculations of the stationary points on the $^3A''$ PES. All values in kcal/mol.

	O–HBr	Transition State	OH–Br	OH+Br
R/UCCSD(T)/AVQZ(-PP)	− 1.49	5.80	− 20.88	− 13.91
R/UCCSD(T)/AV5Z(-PP)	− 1.43	5.86	− 21.04	− 13.96
R/UCCSD(T)/CBS(-PP)	− 1.36	5.92	− 21.20	− 14.02
ΔT	− 0.01	− 0.60	− 3.97	− 0.02
ΔQ	0.00	− 0.15	− 1.16	− 0.06
ΔCV	− 0.05	0.03	0.69	0.42
ΔDK	0.01	− 0.26	− 0.64	− 0.46
ΔSO	0.20	0.07	− 0.25	− 3.29
ΔT+ΔQ+ΔCV+ΔDK+ΔSO	0.15	− 0.91	− 5.33	− 3.41
Best estimate	− 1.21	5.01	− 26.53	− 17.43

TABLE IV. Properties of the saddle points on the scaled and unscaled $^3A''$ and $^3A'$ PESs.

	$^3A''$ (unscaled)	$^3A''$ (scaled)	$^3A'$ (unscaled)	$^3A'$ (scaled)
$r^{\ddagger}_{OH}$ (a_0)	2.608	2.629	2.515	2.537
$r^{\ddagger}_{HBr}$ (a_0)	2.868	2.849	2.877	2.858
$\theta^{\ddagger}_{OHBr}$ (deg.)	135.7	137.5	180.0	180.0
$\Delta^{\ddagger}V$ (kcal/mol)	6.55	5.01	8.04	6.45
$\Delta^{\ddagger}V_0$[a] (kcal/mol)	5.10	3.44	5.67	4.16
$\omega^{\ddagger}_b$ (cm^{-1})	232.1	213.0	469.0	465.0
$\omega^{\ddagger}_s$ (cm^{-1})	1400.6	1339.2	524.5	582.0
$\omega^{\ddagger}_a$ (cm^{-1})	1294.7*i*	1239.4*i*	1495.8*i*	1270.5*i*

[a]Including local and reactant zero-point energies.

TABLE V. Properties of the van der Waals minima on the scaled and unscaled $^3A''$ PESs.

	$^3A''$ (unscaled)	$^3A''$ (scaled)
	O–HBr (Reactant-side well)	
r_{OH} (a_0)	4.477	4.375
r_{HBr} (a_0)	2.685	2.686
θ_{OHBr} (deg.)	180.0	180.0
ΔV (kcal/mol)	− 1.56	− 1.63
ΔV_0 [a] (kcal/mol)	− 1.27	− 1.32
ω_b (cm^{-1})	141.9	153.0
ω_s (cm^{-1})	70.8	74.2
ω_a (cm^{-1})	2635.9	2628.9
	OH–Br (Product-side well)	
r_{OH} (a_0)	1.838	1.837
r_{HBr} (a_0)	4.880	4.822
θ_{OHBr} (deg.)	66.4	67.9
ΔV (kcal/mol)	− 20.96	− 21.05
ΔV_0 [a] (kcal/mol)	− 18.37	− 18.46
ω_b (cm^{-1})	567.3	552.3
ω_s (cm^{-1})	3689.2	3697.0
ω_a (cm^{-1})	206.4	208.4

[a]Including local and reactant zero-point energies.

0.021 a_0, and increases θ_{OHBr} by 1.8° at the transition state on the $^3A''$ PES. Similar changes occur for the geometry of the saddle point on the $^3A'$ surface. The r_{OH} bond length increases by 0.022 a_0 and the r_{HBr} distance decreases by 0.019 a_0, and the barrier height in this electronic state is reduced by 1.59 kcal/mol. The scaling also modifies the harmonic frequencies of the transition states, but not too significantly. The vibrationally adiabatic barrier heights are 3.44 kcal/mol and 4.16 kcal/mol for the $^3A''$ and $^3A'$ PESs, respectively. Table V shows the minor effect of the scaling on the vdW wells on the $^3A''$ PES.

A general overview of the scaled PES for the $^3A''$ electronic state is displayed in Figs. 2, 3, and 4. In these isopotential contour plots, energies (in kcal/mol), relative to the

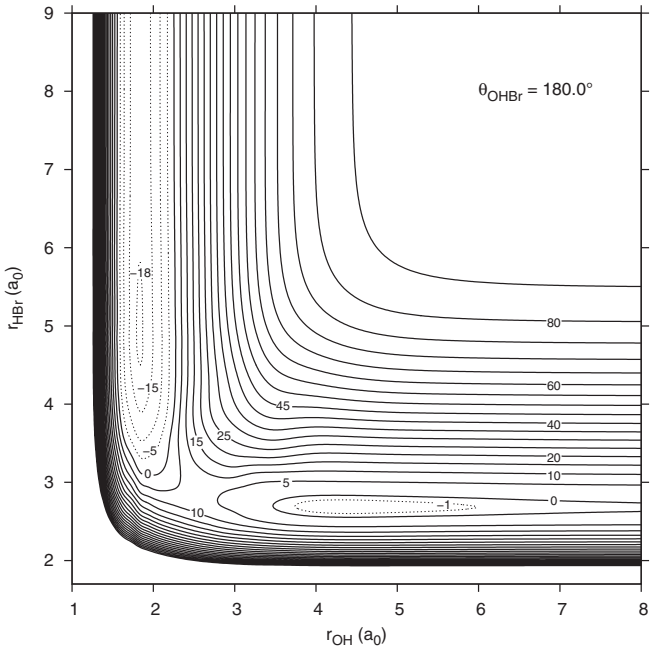

FIG. 2. Equipotential contour plot of the scaled $^3A''$ PES in (r_{OH}, r_{HBr}) space for $\theta_{OHBr} = 180.0°$, corresponding to entrance van der Waals well. The zero of energy is the O + HBr(r_e) asymptotic limit. Negative energies are shown as dotted lines, and the equipotential lines are separated by 5 kcal/mol, unless otherwise noted.

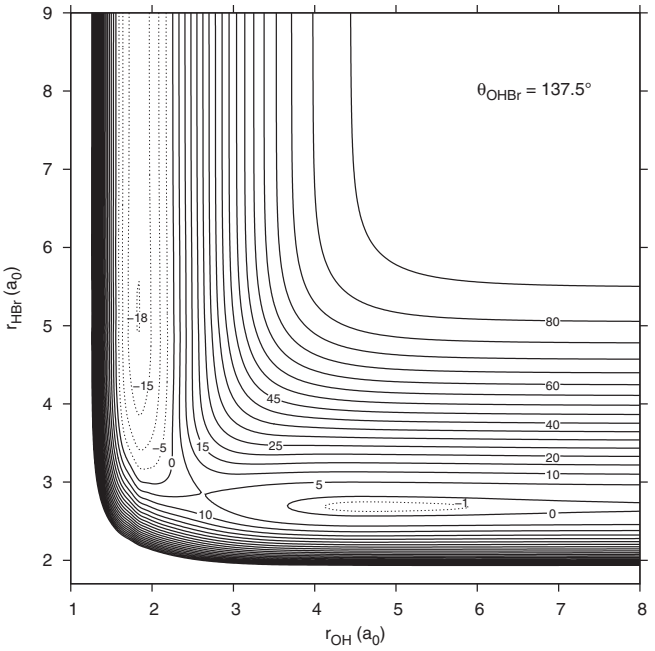

FIG. 3. Equipotential contour plot of the scaled $^3A''$ PES in (r_{OH}, r_{HBr}) space for $\theta_{OHBr} = 137.5°$, corresponding to the transition state. The zero of energy is the O + HBr(r_e) asymptotic limit. Negative energies are shown as dotted lines, and the equipotential lines are separated by 5 kcal/mol, unless otherwise noted.

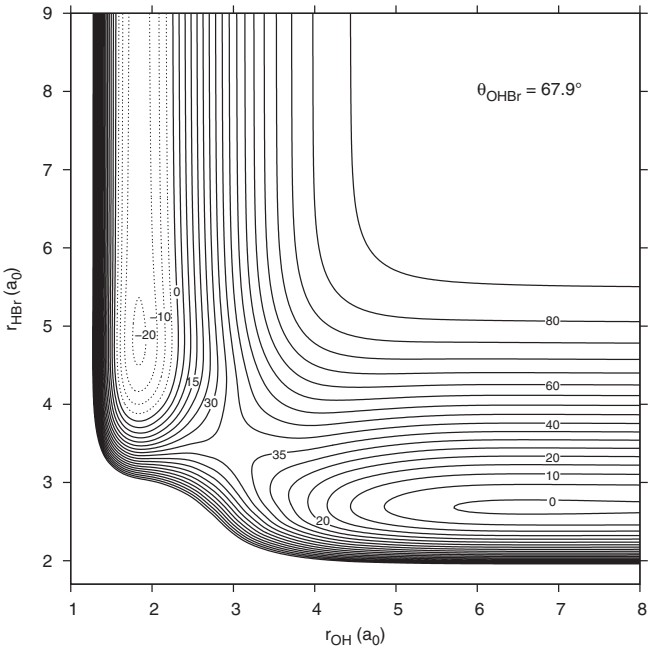

FIG. 4. Equipotential contour plot of the scaled $^3A''$ PES in (r_{OH}, r_{HBr}) space for $\theta_{OHBr} = 67.9°$, corresponding to exit van der Waals well. The zero of energy is the O + HBr(r_e) asymptotic limit. Negative energies are shown as dotted lines, and the equipotential lines are separated by 5 kcal/mol.

$O(^3P) + HBr(r_e)$ asymptotic limit, are shown as a function of r_{OH} and r_{HBr} for a fixed θ_{OHBr}. It is noteworthy to point out that these representations show smooth, well-behaved surfaces, very similar to the ones reported by Ramachandran and Peterson for O + HCl,[15] but using just one three-body potential. In Figure 2 the θ_{OHBr} angle is frozen at the value of 180.0°, corresponding to the entrance vdW minimum, a structure that is easily spotted in the lower part of the plot. The behavior of the surface in this cut is essentially the same for $\theta_{OHBr} = 137.5°$, the value of the equilibrium angle of the transition state, as shown in Figure 3. Figure 4 shows a cut of the scaled $^3A''$ for $\theta_{OHBr} = 67.9°$. This plot is much more repulsive in the reactants side, on the right, as the previous plots, and shows a deep well in the products side, on the left, corresponding to the vdW minimum at the exit channel.

V. SUMMARY

In this paper, we present accurate potential energy surfaces for the triplet OHBr system, focusing on the reaction $O(^3P) + HBr \rightarrow OH + Br$ in the $^3A''$ and $^3A'$ electronic states. The surfaces are based on the many-body expansion with two-body potentials fitted to switched-MLJ functions and three-body potentials interpolated using the RKHS method. The *ab initio* points used to build these functions were obtained at the MRCI+Q/CBS+SO level of theory. The final surface for the $^3A''$ state was scaled in order to reproduce benchmark calculations on its barrier height, and the one for the $^3A'$ PES was scaled to maintain the degeneracy of the two surfaces at the collinear saddle point. The main features of the $^3A''$ PES are a 1.63 kcal/mol deep van der Waals minimum in the entrance channel with a linear geometry, a sharply bent, with $\theta_{OHBr} = 67.9°$, vdW well in the exit channel that is 21.05 kcal/mol lower than the reactants, and a transition state 5.01 kcal/mol higher than the reactants with a vibrationally adiabatic barrier height of 3.44 kcal/mol. The $^3A'$ PES does not have minima and has a linear transition state at 6.45 kcal/mol. Work on dynamical calculations using these PESs is in progress and the results will be reported in a forthcoming paper.

ACKNOWLEDGMENTS

F.R.O. acknowledges the Conselho Nacional de Desenvolvimento Científico e Tecnológico (CNPq) of Brazil for academic support. A.G.S.O.F. is thankful to Fundação de Amparo à Pesquisa do Estado de São Paulo (FAPESP) for a graduate fellowship.

[1] R. P. Wayne, *Chemistry of Atmospheres* (Oxford University Press, 2000).
[2] Y. L. Yung, J. P. Pinto, R. T. Watson, and S. P. Sander, J. Atmos. Sci. **37**, 339 (1980).
[3] G. A. Takacs and G. P. Glass, J. Phys. Chem. **77**, 1182 (1973).
[4] R. D. H. Brown and I. W. M. Smith, Int. J. Chem. Kinet. **7**, 301 (1975).
[5] D. L. Singleton and R. J. Cvetanović, Can. J. Chem. **56**, 2934 (1978).
[6] D. F. Nava, S. R. Bosco, and L. J. Stief, J. Chem. Phys. **78**, 2443 (1983).
[7] J. M. Nicovich and P. H. Wine, Int. J. Chem. Kinet. **22**, 379 (1990).
[8] J. E. Spencer and G. P. Glass, Int. J. Chem. Kinet. **9**, 97 (1977).
[9] K. G. McKendrick, D. J. Rakestraw, and R. N. Zare, Faraday Discuss. **84**, 39 (1987).
[10] K. G. McKendrick, D. J. Rakestraw, R. Zhang, and R. N. Zare, J. Phys. Chem. **92**, 5530 (1988).
[11] M. Brouard and C. Vallance, Phys. Chem. Chem. Phys. **3**, 3602 (2001).
[12] H. Koizumi, G. C. Schatz, and M. S. Gordon, J. Chem. Phys. **95**, 6421 (1991).
[13] B. Ramachandran, J. Senekowitsch, and R. E. Wyatt, Chem. Phys. Lett. **270**, 387 (1997).
[14] B. Ramachandran, E. A. Schrader III, J. Senekowitsch, and R. E. Wyatt, J. Chem. Phys. **111**, 3862 (1999).
[15] B. Ramachandran and K. A. Peterson, J. Chem. Phys. **119**, 9590 (2003).
[16] A. J. Binder, R. Dawes, A. W. Jasper, and J. P. Camden, J. Phys. Chem. Lett. **1**, 2940 (2010).
[17] S. W. Mayer and L. Schieler, J. Phys. Chem. **72**, 236 (1968).
[18] E. J. Shipsey, J. Chem. Phys. **58**, 232 (1973).
[19] M. Broida, M. Tamir, and A. Persky, Chem. Phys. **110**, 83 (1986).
[20] A. Persky and H. Kornweitz, Chem. Phys. **133**, 415 (1989).
[21] J. Urban and V. Staemmler, Chem. Phys. **178**, 279 (1993).
[22] S. P. Sander, J. Abbatt, J. R. Barker, J. B. Burkholder, R. R. Friedl, D. M. Golden, R. E. Huie, C. E. Kolb, M. J. Kurylo, G. K. Moortgat, V. L. Orkin, and P. H. Wine, Chemical kinetics and photochemical data for use in atmospheric studies, evaluation no. 17 (2011), JPL Publication 10-6, Jet Propulsion Laboratory, Pasadena, http://jpldataeval.jpl.nasa.gov.
[23] A. F. Jalbout, J. Mol. Struc. (THEOCHEM) **571**, 103 (2001).
[24] T. Xie, J. M. Bowman, K. A. Peterson, and B. Ramachandran, J. Chem. Phys. **119**, 9601 (2003).
[25] M. P. Deskevich, D. J. Nesbitt, and H.-J. Werner, J. Chem. Phys. **120**, 7281 (2004).
[26] H.-J. Werner and P. J. Knowles, J. Chem. Phys. **82**, 5053 (1985).
[27] P. J. Knowles and H.-J. Werner, Chem. Phys. Lett. **115**, 259 (1985).
[28] H.-J. Werner and P. J. Knowles, J. Chem. Phys. **89**, 5803 (1988).
[29] P. J. Knowles and H.-J. Werner, Chem. Phys. Lett. **145**, 514 (1988).
[30] S. R. Langhoff and E. R. Davidson, Int. J. Quantum Chem. **8**, 61 (1974).
[31] T. H. Dunning, Jr., J. Chem. Phys. **90**, 1007 (1989).
[32] R. A. Kendall, T. H. Dunning, Jr., and R. J. Harrison, J. Chem. Phys. **96**, 6796 (1992).
[33] K. A. Peterson, D. Figgen, E. Goll, H. Stoll, and M. Dolg, J. Chem. Phys. **119**, 11113 (2003).
[34] K. A. Peterson, B. C. Shepler, D. Figgen, and H. Stoll, J. Phys. Chem. A **110**, 13877 (2006).
[35] T. Helgaker, W. Klopper, H. Koch, and J. Noga, J. Chem. Phys. **106**, 9639 (1997).
[36] A. Berning, M. Schweizer, H.-J. Werner, P. J. Knowles, and P. Palmieri, Mol. Phys. **98**, 1823 (2000).
[37] K. Raghavachari, G. W. Trucks, J. A. Pople, and M. Head-Gordon, Chem. Phys. Lett. **157**, 479 (1989).
[38] J. D. Watts, J. Gauss, and R. J. Bartlett, J. Chem. Phys. **98**, 8718 (1993).
[39] P. J. Knowles, C. Hampel, and H.-J. Werner, J. Chem. Phys. **99**, 5219 (1993).
[40] J. Noga and R. J. Bartlett, J. Chem. Phys. **86**, 7041 (1987).
[41] G. E. Scuseria and H. F. Schaefer III, Chem. Phys. Lett. **152**, 382 (1988).
[42] M. Kállay and P. R. Surján, J. Chem. Phys. **115**, 2945 (2001).
[43] A. K. Wilson, D. E. Woon, K. A. Peterson, and T. H. Dunning, Jr., J. Chem. Phys. **110**, 7667 (1999).
[44] S. A. Kucharski and R. J. Bartlett, Theor. Chim. Acta **80**, 387 (1991).
[45] S. A. Kucharski and R. J. Bartlett, J. Chem. Phys. **97**, 4282 (1992).
[46] N. Oliphant and L. Adamowicz, J. Chem. Phys. **95**, 6645 (1991).
[47] K. A. Peterson and T. Dunning, Jr., J. Chem. Phys. **117**, 10548 (2002).
[48] K. A. Peterson and K. E. Yousaf, J. Chem. Phys. **133**, 174116 (2010).
[49] M. Douglas and N. M. Kroll, Ann. Phys. **82**, 89 (1974).
[50] W. A. de Jong, R. J. Harrison, and D. A. Dixon, J. Chem. Phys. **114**, 48 (2001).
[51] H.-J. Werner, P. J. Knowles, F. R. Manby, M. Schütz *et al.*, MOLPRO, version 2010.1, a package of *ab initio* programs, 2010, see http://www.molpro.net.
[52] MRCC, a string-based quantum chemical program suite written by M. Kállay. See also Ref. 42 as well as http://www.mrcc.hu.
[53] K. S. Sorbie and J. N. Murrell, Mol. Phys. **29**, 1387 (1975).
[54] A. J. C. Varandas and J. N. Murrell, Faraday Discuss. **62**, 92 (1977).

[55]J. N. Murrell, S. Carter, S. C. Farantos, P. Huxley, and A. J. C. Varandas, *Molecular Potential Energy Functions* (Wiley, New York, 1984).
[56]P. G. Hajigeorgiou and R. J. Le Roy, J. Chem. Phys. **112**, 3949 (2000).
[57]T.-S. Ho and H. Rabitz, J. Chem. Phys. **104**, 2584 (1996).
[58]T. Hollebeek, T.-S. Ho, and H. Rabitz, J. Chem. Phys. **106**, 7223 (1997).
[59]K. P. Huber and G. Herzberg, *Molecular Spectra and Molecular Structure IV. Constants of Diatomic Molecules* (Van Nostrand Reinhold, New York, 1979).
[60]B. Ruscic, A. F. Wagner, L. B. Harding, R. L. Asher, D. Feller, D. A. Dixon, K. A. Peterson, Y. Song, X. Qian, C.-Y. Ng, J. Liu, W. Chen, and D. W. Schwenke, J. Phys. Chem. A **106**, 2727 (2002).
[61]E. A. Shenyavskaya and V. S. Yungman, J. Phys. Chem. Ref. Data **33**, 923 (2004).
[62]B. J. Drouin, C. E. Miller, H. S. Müller, and E. A. Cohen, J. Mol. Spectrosc. **205**, 128 (2001).
[63]H. Kim, K. S. Dooley, E. R. Johnson, and S. W. North, J. Chem. Phys. **124**, 134304 (2006).